https://doi.org/10.48048/tis.2023.6147

Heterophase of Bismuth Titanate as a Photocatalyst for Rhodamine B Degradation

Atiek Rostika Noviyanti[1,*], Diana Rakhmawaty Eddy[1], Muhamad Diki Permana[1,2,3] and Risdiana[4]

[1]Department of Chemistry, Faculty Mathematics and Natural Sciences, Universitas Padjadjaran Sumedang, West Java 45363, Indonesia
[2]Integrated Graduate School of Medicine, Engineering and Agricultural Sciences, University of Yamanashi, Kofu 4008511, Japan
[3]Center for Crystal Science and Technology, University of Yamanashi, Kofu 4008511, Japan
[4]Department of Physics, Faculty Mathematics and Natural Sciences, Universitas Padjadjaran Sumedang, West Java 45363, Indonesia

([*]Corresponding author's e-mail: atiek.noviyanti@unpad.ac.id)

Received: 29 September 2022, Revised: 29 November 2022, Accepted: 6 December 2022, Published: 20 August 2023

Abstract

Various studies have been made to obtain high efficiency photocatalysts. Auvirillius bismuth titanate oxide is known to have good photocatalytic activity to degrade dyestuffs. However, recombination is still an obstacle to photocatalytic efficiency. To overcome recombination and increase photocatalytic activity, it is proposed to synthesize bismuth titanate heterophase. Heterophase can enhance the formation of the synergistic effect of electrons, which effectively stimulates the transfer of electrons from 1 phase to another. This study aims to determine the photocatalytic ability of bismuth titanate heterophase for degradation of a rhodamine B. Bismuth titanate was synthesized by hydrothermal method using Bi_2O_3 and TiO_2 precursors. The results of X-ray diffraction characterization showed that the synthesized bismuth titanate formed 2 phases, namely $Bi_4Ti_3O_{12}$ (78.2 %) and $Bi_{12}Ti_{0.9}O_{19.8}$ (21.8 %). In addition, it is also known that the volume of the synthesized bismuth titanate crystal lattice has a smaller volume than the standard synthesized in previous studies. The photocatalytic ability of bismuth titanate evaluated using 10 mg/L rhodamine B showed that it took 240 min to degrade 98 % of dye. Reaction kinetics studies showed that bismuth titanate has a reaction rate constant efficiency of 120 % better than TiO_2 for the Langmuir- Hinshelwood 1st-order kinetic model. Then the reuse ability was evaluated, showing that after 3 times of uses, bismuth titanate only decreased 5 %, whereas TiO_2 decreased by 7 % in degradation.

Keywords: Metal oxide, Degradation, Photocatalysis, Wastewater treatment

Introduction

The rapid development of the textile industry has become one of the largest contributors of dye waste to the environment [1]. Dyestuff waste causes aesthetic problems and organic pollutants that have a negative impact on aquatic organisms and humans [2]. One of the dyes used is rhodamine B [3]. Rhodamine B or also called tetraethyl rhodamine is a basic organic dye. Rhodamine B can cause irritation to the skin, eyes, respiratory tract and digestive tract. While in the body it can cause various serious diseases such as liver cancer and kidney damage [4]. Thus, the presence of rhodamine B dye should be reduced in the environment. Currently, many methods have been used to reduce rhodamine B levels, namely sonolysis [3,5], Fenton method [6,7], ozonolysis [8], and photocatalysis [9,10]. In recent years, photocatalysis has become a frequently used method [11-13]. Photocatalysis is used because it has advantages, namely high degradation efficiency [14], low cost, and environmentally friendly [15].

Metal oxides are one of the most important types of materials, apart from the fact that minerals or metallic ores are found in nature in the form of metal oxides [16], and also because of their many cutting-edge uses such as superconducting materials [17,18] and catalysts [19-21]. The diversity of applications in metal oxides comes from the diversity of the structure and properties of the metal oxides [22]. This is the reason why research on metal oxide materials continues to be carried out. Over the past 4 decades, various metal oxides have been used in photocatalysis. One of the most frequently used materials is TiO_2. TiO_2 is widely used because it has good chemical stability and is relatively cheap in price [14]. However, the photoactivity of TiO_2 has the disadvantage that it only absorbs a small part of the solar spectrum and there

is still a lot of hole-electron recombination [23]. Lee *et al*. [24] mentioned that TiO_2 has limited photocatalytic efficiency due to its wide energy bandgap. It takes alternative materials that have small bandgap energy.

Bismuth titanate is the Aurivillius family of compounds. Bismuth titanate has a band gap energy of 2.88 eV, which is lower than TiO_2 of 3.24 eV [25]. This compound consists of a perovskite layer $[Bi_3Ti_3O_{10}]^{2-}$ which is intercalated with 2 layers of $[Bi_2O_2]^{2+}$. The electric field between the $(Bi_2O_2)^{2+}$ layer and the $(Bi_2Ti_3O_{10})^{2-}$ layer can prevent the recombination of holes and electrons and can increase photocatalytic activity [26]. Thus, in this study bismuth titanate was used as a photocatalyst material. In addition, to increase the photocatalytic ability, heterophase modification is also used. Heterophase can enhance the formation of a synergistic effect of electrons, which effectively stimulates the transfer of electrons from 1 phase to another [27].

Bismuth titanate has been synthesized using various methods, including solid chemical reaction, coprecipitation and sol-gel. In recent years, it has been reported that the hydrothermal method is used to synthesize $Bi_4Ti_3O_{12}$ [28]. The hydrothermal method has several advantages such as allowing the synthesis of compounds that have oxidation numbers that are difficult to obtain, metastable compounds and obtainable high purity [29].

Therefore, in this study, bismuth titanate was synthesized as a photocatalyst for the degradation of rhodamine B. TiO_2 and Bi_2O_3 were used as precursors for the synthesis of bismuth titanate. In addition, the synthesis was carried out using the hydrothermal method and made into a heterophase which makes this research different from previous studies. The properties of the bismuth titanate crystals formed were examined by XRD. We also compared the photocatalytic activity of synthesized bismuth titanate with TiO_2. In addition, the reusability of its photocatalytic activity on the decomposition of rhodamine B was also investigated.

Materials and methods

Materials

The materials used in this study are bismuth oxide (Bi_2O_3, 99.99 %, Sigma-Aldrich, St. Louis, USA), titanium dioxide (TiO_2 Anatase, ≥ 90 %, Sigma-Aldrich, St. Louis, USA), demineralized aqua (Brataco, Tangerang, Indonesia), sodium hydroxide (NaOH, 99.99 %, Merck, Kenilworth, USA), and rhodamine B ($C_{28}H_{31}ClN_2O_3$, 99.99 %, Merck, Kenilworth, USA).

Synthesis of bismuth titanate by hydrothermal method

Bismuth titanate was synthesized by hydrothermal method. Bismuth oxide (Bi_2O_3), titanium dioxide (TiO_2) were mixed in a mole ratio of 2:3. Then the mixture was dissolved in 50 mL of 3 M NaOH, put into an autoclave (CIT-HTC230-V100 Co1-Int 125 mL) and heated in an oven at 240 °C for 72 h. The product formed was washed with demineralized water, and then filtered and dried in an oven at 110 °C for 18 h. A yellowish-white bismuth titanate was produced (**Figure 1**) with a yield of 92 %.

Figure 1 Bismuth titanate has been synthesized to produce a yellowish-white powder.

Characterization of bismuth titanate

The resulting bismuth titanate was further characterized by using X-ray diffraction (XRD) to identify the structure of crystals. Bismuth titanate was analyzed by XRD (PANalytical type X'Pert PRO PW 3040/x0). Measurements were carried out at room temperature using Cu Kα radiation at an angle of 2θ from 10 to 80 °. Crystal structure was refined by Rietveld refinement using HighScore Plus (PANalytical 3.0.5)

software [30]. The refinement result of the crystal is drawn using the Visualization for Electronic Structural Analysis (VESTA) software.

Photocatalytic activity test of bismuth titanate

A total of 50 mg of sample and 50 mL of rhodamine B 10 ppm were mixed in a beaker. The mixture was then placed in a homemade photoreactor and irradiated with a Hg lamp (HPL-N 125W, Philips, China, UV A equivalent to a wavelength of 315 - 400 nm) on a magnetic stirrer (IKA C-MAG MS 4, Germany) with an irradiation area of 26 cm^2 for 4 h at room temperature. Then, 2 mL of rhodamine B solution was taken every 1 h using a membrane syringe. Rhodamine B solution then analyzed using UV-vis spectrophotometer (Genesys 10S, USA) to determine the remaining concentration of rhodamine B. For the reuse study, after use, the catalyst was centrifuged and then dried in an oven at 110 °C for 18 h. Then, the catalyst was used again to see its ability to degrade rhodamine B.

Results and discussion

Structural analysis of bismuth titanate by XRD

The results of the X-ray diffraction (XRD) analysis are shown in **Figure 2**. The XRD pattern of bismuth titanate shows similarities to the Inorganic Crystal Structure Database (ICSD) 98-015-9929 for $Bi_4Ti_3O_{12}$ (orthorhombic, space group *A*ba2) [31], and ICSD 98-003-9288 for $Bi_{12}Ti_{0.9}O_{19.8}$ (cubic, space group *I*23) [32]. $Bi_4Ti_3O_{12}$ shows peak patterns at 2θ = 23.3° (111), 30.1° (171), 32.8° (002) and several other peaks. Whereas at 2θ = 24.7 and 27.7° which correspond to (022) and (013) atomic planes, respectively, are typical peaks of $Bi_{12}Ti_{0.9}O_{19.8}$.

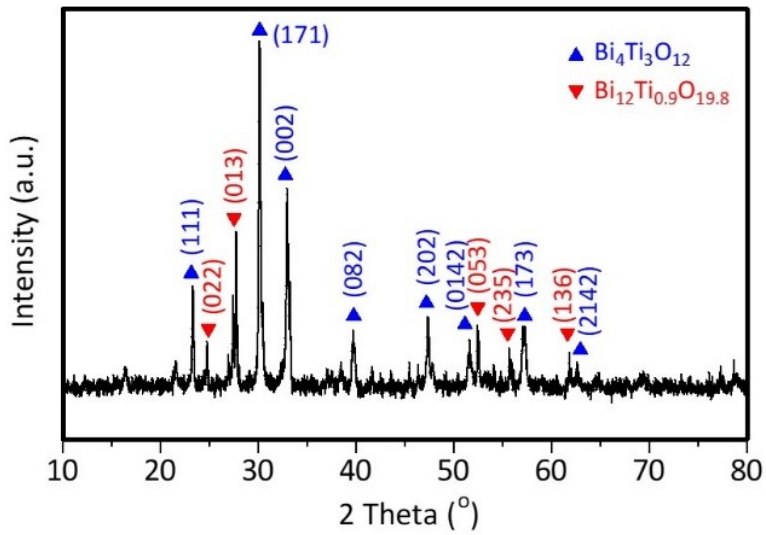

Figure 2 Diffraction pattern of bismuth titanate synthesized by hydrothermal method.

The percentage of synthesized bismuth titanate crystal structure was calculated using the Rietveld method and refined using the HighScore Plus software (PANalytical 3.0.5) [30]. Scale-factors, 0-shift, and coefficients of shifted polynomial functions are used to match the background. **Table 1** shows the percentage of the Rietveld refinement phase, where the synthesis results show that 2 phases are formed, namely $Bi_4Ti_3O_{12}$ of 78.2 % and $Bi_{12}Ti_{0.9}O_{19.8}$ of 21.8 %. Thus, it can be seen that the hydrothermal method causes the formation of 2 phases of bismuth titanate, where defects occur in the minor phase. The crystal structure of bismuth titanate as shown in **Figure 3**.

Table 1 Phase percentages and Rietveld refinement parameters of the samples.

Phase	ICSD	Phase Percentage (%)	Rp	Rwp	Rexp	GoF
$Bi_4Ti_3O_{12}$	98-015-9929	78.2	7.706	10.450	7.208	2.102
$Bi_{12}Ti_{0.9}O_{19.8}$	98-003-9288	21.8				

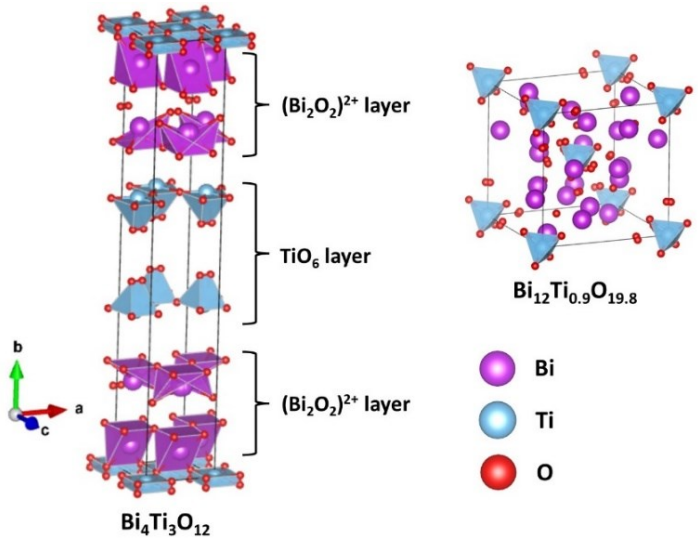

Figure 3 Crystal structure of $Bi_4Ti_3O_{12}$ and $Bi_{12}Ti_{0.9}O_{19.8}$.

To confirm the accuracy of the calculation from Rietveld refinement, the goodness of fit (GoF) value of the experimental XRD pattern is also calculated with the XRD pattern calculated from the standard (**Figure 4**). GoF is a statistical model describing how well the experimental results were obtained with a series of observations [33]. The smaller the GoF value, the better the match, with the ideal GoF value being 1 [34]. In **Table 1**, it can be seen that the GoF value in the sample is 2.102, which is still acceptable.

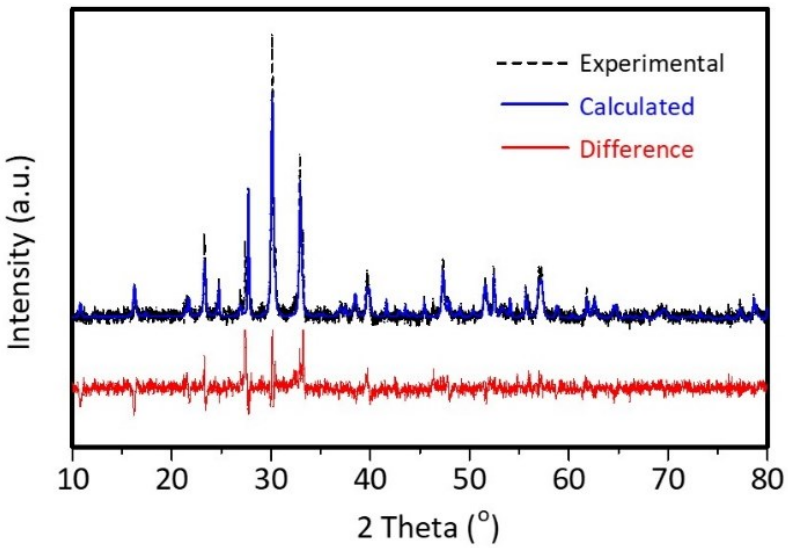

Figure 4 Plot of the result of fitting Rietveld refinement of XRD pattern of bismuth titanate.

Crystal size was calculated using the Debye-Scherrer equation. The calculated crystal size is the average of each phase peak in the XRD pattern. The crystal size of the sample was calculated by Eq. (1) [35].

$$D = (K \lambda)/(B \cos\theta) \quad (1)$$

where D is the crystal size (nm), K is the Scherrer constant (0.89), B is the peak full width at half maximum (FWHM) value (rad), is the wavelength of X-ray radiation (0.15418 nm), and is the diffraction angle (rad). **Table 2** shows that the crystal size of the $Bi_4Ti_3O_{12}$ phase has a smaller size of 32.31 nm, compared to the $Bi_{12}Ti_{0.9}O_{19.8}$ phase of 64.86 nm.

Table 2 The crystal size and crystallinity percentages of the samples.

Phase	Crystal size (mean ± standard deviation)	Crystallinity
$Bi_4Ti_3O_{12}$	32.31 ± 4.69 nm	82.63
$Bi_{12}Ti_{0.9}O_{19.8}$	64.86 ± 4.67 nm	

The crystallinity of the sample was calculated by comparing the peaks of the crystal phase with the total peaks in the XRD pattern using the OriginPro 8.5.1 SR2 software [36]. **Table 2** shows the crystallinity percentage of the samples. It can be seen that the crystallinity of the synthesized bismuth titanate has a large crystallinity. Large crystallinity is needed in photocatalysis in order to avoid the possibility of electron-hole recombination so that it can increase photocatalytic activity [37,38].

Table 3 shows the lattice parameters of bismuth titanate samples and ICSD standards. It can be seen that the synthesized substance has bismuth titanate crystals with a volume smaller than the ICSD standard. The difference in the volume of the $Bi_4Ti_3O_{12}$ crystal lattice is 0.888 $Å^3$, while the different volume of the $Bi_{12}Ti_{0.9}O_{19.8}$ crystal lattice is 5.950 $Å^3$. This shows that the bismuth titanate synthesis process using the hydrothermal method produces a smaller crystal lattice than other methods that have been carried out previously [31,32].

Table 3 The crystal lattice parameters of sample and standard.

Sample	Lattice parameters (Å)			Crystal volume ($Å^3$)
	a	***b***	***c***	
ICSD 98-015-9929	5.426	32.683	5.437	964.190
$Bi_4Ti_3O_{12}$	5.409	32.705	5.445	963.302
ICSD 98-003-9288	10.186	10.186	10.186	1056.840
$Bi_{12}Ti_{0.9}O_{19.8}$	10.167	10.167	10.167	1050.890

Photocatalytic activity of bismuth titanate

The synthesized bismuth titanate was tested for its photocatalytic activity against rhodamine B. TiO_2 was used as a comparison of photocatalytic performance. The experimental results of the photocatalytic degradation of rhodamine B are shown in **Figure 5**. The photocatalyst activity exposed to UV light had a better percentage of degradation (**Figure 5**(**a**)) than that which was not exposed (**Figure 5**(**b**)). This indicates that photons from UV light have a positive effect on photocatalyst performance in the oxidation of rhodamine B. In addition, it is seen that bismuth titanate has better adsorption which is correlated with its photocatalytic ability (97.96 %) for 240 min. Meanwhile, TiO_2 has slightly weaker adsorption and photocatalytic abilities. However, TiO_2 degrades faster during the 1st 120 min of photocatalysis. The data of the phenol concentration and percentage reduction at any time are presented in **Table 4**.

Table 4 Concentration and percentage of rhodamine B removal over time.

Time (min)	Concentration of rhodamine B (mg/L)		Degradation (%)	
	Bismuth titanate	**TiO_2**	**Bismuth titanate**	**TiO_2**
0	10.00 ± 0.40	10.00 ± 0.40	0	0
60	3.94 ± 0.38	1.40 ± 0.26	60.64	85.99
120	2.85 ± 0.24	0.78 ± 0.35	71.53	92.24
180	0.58 ± 0.14	0.53 ± 0.14	94.20	94.71
240	0.20 ± 0.02	0.28 ± 0.05	97.96	97.17

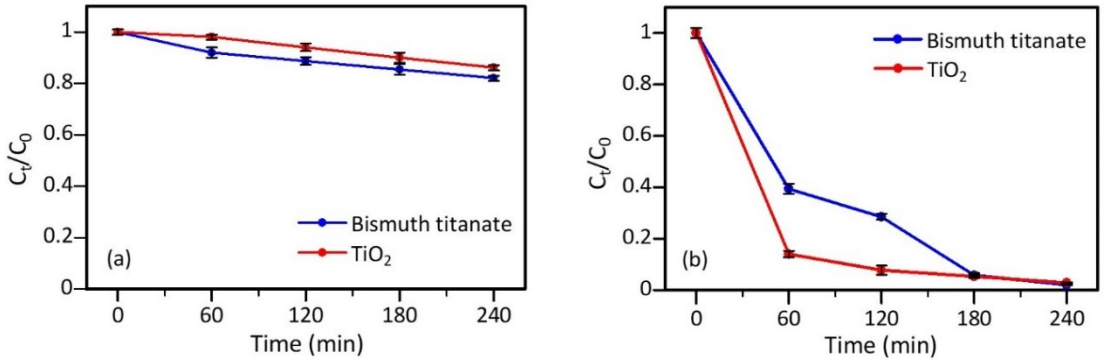

Figure 5 (a) Adsorption activity and (b) Photocatalytic activity of the catalyst against rhodamine B. The experiment was carried out using 50 mL of rhodamine B 10 mg/L with 50 mg of catalyst.

The photocatalyst showed a higher percentage reduction. This shows that the degradation performance of rhodamine B is affected by photons from UV light. Bismuth titanate exposed to UV light will result in a jump of electrons from the valence band to the conduction band. As a result, holes (h^+) and electrons (e^-) are formed. This species reacts with oxygen (O_2) and water (H_2O) from the environment to produce •OH radicals which can degrade rhodamine B. Meanwhile, for those who are not exposed to light (dark state), there is no energy to activate the photocatalyst performance. The process of decreasing the concentration of rhodamine B is an adsorption process. The photocatalytic reactions that occur are described by reactions (2) - (7) [38]:

$$Bi_4Ti_3O_{12} + hv \rightarrow e^- + h^+ \quad (2)$$

$$e^- + O_2 \rightarrow O_2^- \quad (3)$$

$$h^+ + H_2O \rightarrow \bullet OH + H^+ \quad (4)$$

$$O_2^- + 2H^+ \rightarrow \bullet OH + OH^- \quad (5)$$

$$\text{rh B} + O_2^- \rightarrow \text{degradation products} \quad (6)$$

$$\text{rh B} + \bullet OH \rightarrow \text{degradation products} \quad (7)$$

The crystal structure of $Bi_4Ti_3O_{12}$ is composed of 3 TiO_6 octahedral layers and a $(Bi_2O_2)^{2+}$ layer. The electric field between the $(Bi_2O_2)^{2+}$ layer and the $(Bi_2Ti_3O_{10})^{2-}$ layer can prevent the recombination of holes and electrons so as to increase photocatalytic activity. The time required to degrade rhodamine B is slightly longer than that of methyl orange [26]. This can be caused by the structure of rhodamine B which has many aromatic rings and its larger molecular size [39] which makes it more difficult to degrade.

Kinetic studies

The kinetics of the photocatalysis was observed using Langmuir-Hinshelwood 1st order kinetic model. The kinetic model was calculated using [11]:

$$\ln\left(\frac{C_t}{C_i}\right) = -kt + b \quad (8)$$

where C_t represents concentration (mg/L) of rhodamine B at t min, C_i represents initial concentration (mg/L) of rhodamine B, b represents a constant, and k_1 (1/min) is the rate constant.

Figure 6 shows the kinetic model listed in **Table 5**. As shown in **Table 5**, bismuth titanate has a greater reaction kinetic constant than TiO_2. The k_1 value of bismuth titanate is 0.0162 1/min, with a correlation coefficient of 0.9637 which indicates that the kinetic model used is appropriate [40]. Compared to TiO_2, bismuth titanate has a reaction efficiency of 120 % better from the value of the rate constant.

Table 5 Parameters of kinetic models.

Sample	Langmuir-Hinshelwood 1st order	
	k_1 (1/min)	R^2
Bismuth titanate	0.0162	0.9637
TiO_2	0.0135	0.8838

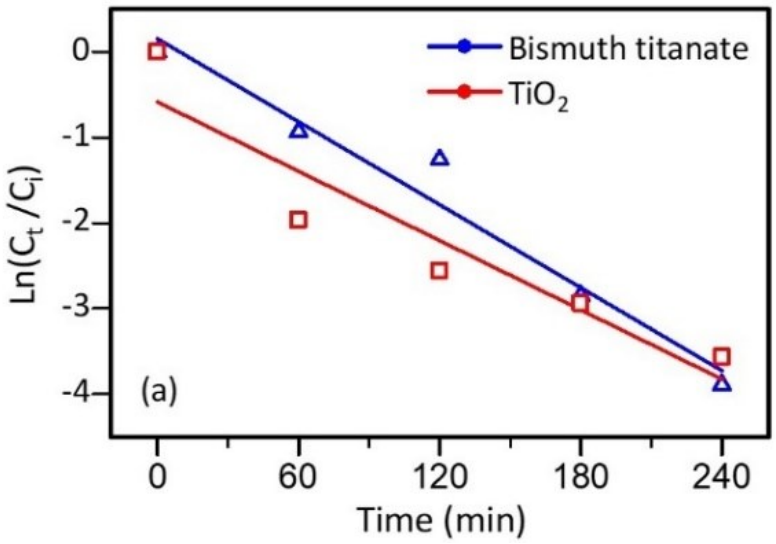

Figure 6 Kinetic models for Langmuir-Hinshelwood 1st-order linear of rhodamine B degradation.

The catalytic activity in the photodegradation of rhodamine B is compared with the data that have been reported in the literature shown in **Table 6**, clearly showing that our data on photoactivity are compared with those published in the literature. The presence of heterophase can enhance the formation of electron synergistic effect, which effectively stimulates electron transfer from 1 phase to another [27].

Table 6 Comparison of various bismuth titanate photocatalytic activity with several previous reports in rhodamine B degradation.

Materials	Initial concentration of rhodamine B	Irradiation time (min)	Reaction constant (min^{-1})	Ref.
$Bi_4Ti_3O_{12}$	10 mg/L	210 min	0.01400	[41]
$Bi_{12}TiO_{20}$	10 mg/L	210 min	0.01990	[41]
$Bi_2Ti_2O_7$ nanorods	10 mg/L	120 min	-	[42]
$Bi_4Ti_3O_{12}$ nanosheets	6 mg/L	90 min	-	[43]
Bi_2WO_6	1.0×10^{-5} M	180 min	0.00476	[44]
$Bi_4Ti_3O_{12}/Bi_{12}Ti_{0.9}O_{19.8}$	10 mg/L	240 min	0.01620	This work

Reusability

The stability of the photocatalyst during photoreaction is an important factor for practical applications. The stability test was investigated by carrying out a recycling reaction for photocatalysis of rhodamine B under light irradiation. The dried bismuth titanate was given the same treatment as before. **Figure 7** shows that in the 1st round, the degradation ability is 98 %, after 3 times of use, the degradation ability is 93 %. This means that bismuth titanate composite has only decreased by 5 %. As for the TiO_2 photocatalyst, the degradation ability decreased by more, namely 7 %. In conclusion, synthesized bismuth titanate has a better potential to be developed as a commercial catalyst.

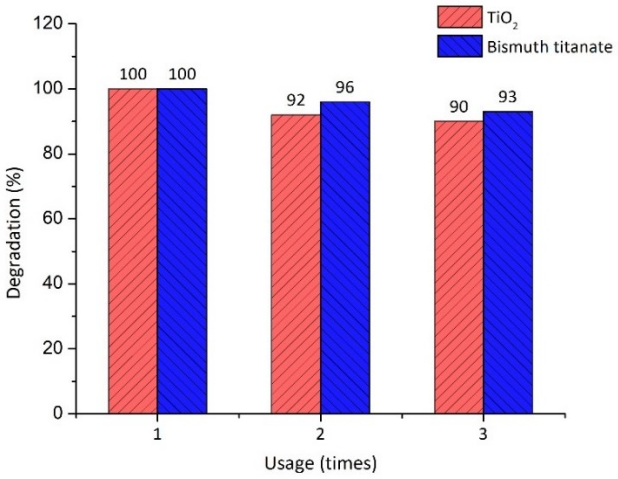

Figure 7 Graph of the reuse capability of bismuth titanate and TiO_2 photocatalysts with 240 min degradation of 10 mg/L of rhodamine B.

Conclusions

In this study, photocatalytic degradation of rhodamine B was carried out using bismuth titanate heterophase. Heterophase bismuth titanate was synthesized using the hydrothermal method from precursors Bi_2O_3 and TiO_2. The results showed 2 phases: The $Bi_4Ti_3O_{12}$ phase had a percentage of 78.2 % and the $Bi_{12}Ti_{0.9}O_{19.8}$ phase of 21.8 %. It is also known that $Bi_4Ti_3O_{12}$ has a smaller crystal size than $Bi_{12}Ti_{0.9}O_{19.8}$. In addition, bismuth titanate crystals have a smaller lattice volume than the standard from the previous literature. The percentage decrease in the concentration of rhodamine B with bismuth titanate heterophase is 99 % within 240 min and 120 % more efficient than TiO_2. From the ability to reuse, after 3 runs, bismuth titanate heterophase only had a 5 % decrease in degradation ability. These results indicate that bismuth titanate heterophase can be used as a new approach to remove rhodamine B compounds in wastewater.

Acknowledgements

The authors are grateful to Universitas Padjadjaran who has funded this work under Academic Leadership Grant (ALG) through project number 2203/UN6.3.1/PT.00/2022

References

[1] K Singh, P Kumar and R Srivastava. An overview of textile dyes and their removal techniques: Indian perspective. *Pollut. Res.* 2017; **36**, 790-7.

[2] H Zhao, G Zhang, S Chong, N Zhang and Y Liu. MnO_2/CeO_2 for catalytic ultrasonic decolorization of methyl orange: Process parameters and mechanisms. *Ultrason. Sonochem.* 2015; **27**, 474-9.

[3] S Merouani, O Hamdaoui, F Saoudi and M Chiha. Sonochemical degradation of rhodamine B in aqueous phase: Effects of additives. *Chem. Eng. J.* 2010; **158**, 550-7.

[4] AG Pierce and RB Neil. *At a glance ilmu bedah* (*in Indonesian*). Erlangga, Jakarta, 2007.

[5] C Lops, A Ancona, K Di Cesare, B Dumontel, N Garino, G Canavese, S Hérnandez and V Cauda. Sonophotocatalytic degradation mechanisms of Rhodamine B dye via radicals generation by micro- and nano-particles of ZnO. *Appl. Catal. B: Environ.* 2019; **243**, 629-40.

[6] MF Hou, L Liao, WD Zhang, XY Tang, HF Wan and GC Yin. Degradation of rhodamine B by Fe(0)-based Fenton process with H_2O_2. *Chemosphere* 2011; **83**, 1279-83.

[7] S Guo, Z Yang, Z Wen, H Fida, G Zhang and J Chen. Reutilization of iron sludge as heterogeneous Fenton catalyst for the degradation of rhodamine B: Role of sulfur and mesoporous structure. *J. Colloid Interface Sci.* 2018; **532**, 441-8.

[8] P Zawadzki and M Deska. Degradation efficiency and kinetics analysis of an Advanced Oxidation Process utilizing ozone, hydrogen peroxide and persulfate to degrade the dye rhodamine B. *Catalysts* 2021; **11**, 974.

[9] F Alakhras, E Alhajri, R Haounati, H Ouachtak, AA Addi and TA Saleh. A comparative study of photocatalytic degradation of rhodamine B using natural-based zeolite composites. *Surf. Interfaces* 2020; **20**, 100611.
[10] A Boughelout, R Macaluso, M Kechouane and M Trari. Photocatalysis of rhodamine B and methyl orange degradation under solar light on ZnO and Cu_2O thin films. *React. Kinet. Mech. Catal.* 2020; **129**, 1115-30.
[11] DR Eddy, SN Ishmah, MD Permana and ML Firdaus. Synthesis of titanium dioxide/silicon dioxide from beach sand as photocatalyst for Cr and Pb remediation. *Catalysts* 2020; **10**, 1248.
[12] DP Bui, HH Pham, TM Cao and VV Pham. Preparation of conjugated polyvinyl chloride/TiO_2 nanotubes for rhodamine B photocatalytic degradation under visible light. *J. Chem. Tech. Biotechnol.* 2020; **95**, 2707-14.
[13] E Fenelon, DP Bui, HH Tran, SJ You, YF Wang, TM Cao and VV Pham. Straightforward synthesis of SnO_2/Bi_2S_3/BiOCl–$Bi_{24}O_{31}C_{l10}$ composites for drastically enhancing rhodamine B photocatalytic degradation under visible light. *ACS Omega* 2020; **5**, 20438-49.
[14] R Ameta and SC Ameta. *Photocatalysis: Principles and applications*. Crc Press, Florida, 2016.
[15] MN Chong, B Jin, CWK Chow and C Saint. Recent developments in photocatalytic water treatment technology: A review. *Water Res.* 2010; **44**, 2997-3027.
[16] P Matteazzi and GL Caër. Synthesis of nanocrystalline alumina-metal composites by room-temperature ball-milling of metal oxides and aluminum. *J. Am. Ceram. Soc.* 1992; **75**, 2749-55.
[17] Y Li, Y Weng, J Zhang, J Ding, Y Zhu, Q Wang, Y Yang, Y Cheng, Q Zhang, P Li, J Lin, W Chen, Y Han, X Zhang, L Chen, X Chen, J Chen, S Dong, X Chen and T Wu. Observation of superconductivity in structure-selected Ti_2O_3 thin films. *NPG Asia Mater.* 2018; **10**, 522-32.
[18] L Si, W Xiao, J Kaufmann, JM Tomczak, Y Lu, Z Zhong and K Held. Topotactic hydrogen in nickelate superconductors and akin infinite-layer oxides ABO_2. *Phys. Rev. Lett.* 2020; **124**, 166402.
[19] JC Védrine. Heterogeneous catalysis on metal oxides. *Catalysts* 2017; **7**, 341.
[20] J Pan, XL Tian, S Zaman, Z Dong, H Liu, HS Park and BY Xia. Recent progress on transition metal oxides as bifunctional catalysts for lithium-air and zinc-air batteries. *Batter. Supercaps* 2019; **2**, 336-47.
[21] PS Palukuru, AV Devangam and DK Behara. N,S-codoped TiO_2/Fe_2O_3 heterostructure assemblies for electrochemical degradation of crystal violet dye. *Iran. J. Chem. Chem. Eng.* 2020; **39**, 171-80.
[22] Ismunandar. *Padatan oksida logam* (*in Indonesian*). ITB Publisher, Bandung, Indonesia, 2006.
[23] SM Park, A Razzaq, YH Park, S Sorcar, Y Park, CA Grimes and SI In. Hybrid Cu_xO-TiO_2 heterostructured composites for photocatalytic CO_2 reduction into methane using solar irradiation: Sunlight into fuel. *ACS Omega* 2016; **1**, 868-75.
[24] MS Lee, SS Hong and M Mohseni. Synthesis of photocatalytic nanosized TiO_2-Ag particles with sol-gel method using reduction agent. *J. Mol. Catal. A: Chem*. 2005; **242**, 135-40.
[25] S Murugesan and VR Subramanian. Robust synthesis of bismuth titanate pyrochlore nanorods and their photocatalytic applications. *Chem. Commun.* 2009; **34**, 5109.
[26] WF Yao, H Wang, XH Xu, SX Shang, Y Hou, Y Zhang and M Wang. Synthesis and photocatalytic property of bismuth titanate $Bi_4Ti_3O_{12}$. *Mater. Lett.* 2003; **57**, 1899-902.
[27] X Wei, S Shao, X Ding, W Jiao and Y Liu. Degradation of phenol with heterogeneous catalytic ozonation enhanced by high gravity technology. *J. Clean. Prod.* 2020; **248**, 119179.
[28] M Rizal and I Ismunandar. Synthesis of Aurivillius $Bi_4Ti_3O_{12}$ using hydrothermal method and structured compound characterization. *J. Mater. Sains* 2009; **12**, 44.
[29] JN Lalena, DA Cleary, E Carpenter and NF Dean. *Inorganic materials synthesis and fabrication.* Wiley-Interscience, New Jersey, 2008.
[30] T Degen, M Sadki, E Bron, U König and G Nénert. The highscore suite. *Powder Diffr.* 2014; **29**, S13-S18.
[31] A Shrinagar, A Garg, R Prasad and S Auluck. Phase stability in ferroelectric bismuth titanate: A first-principles study. *Acta Crystallogr. A* 2008; **64**, 368-75.
[32] SF Radaev and VI Simonov. Structures of sillenites and atomic mechanisms of their isomorphic substitutions. *Sov. Phys. Crystallogr.* 1992; **37**, 484-99.
[33] A Maydeu-Olivares and C Garcia-Forero. Goodness-of-fit testing. *Int. Encycl. Educ.* 2010; **7**, 190-6.
[34] BH Toby. R factors in Rietveld analysis: How good is good enough? *Powder Diffr.* 2006; **21**, 67-70.
[35] DR Eddy, SN Ishmah, MD Permana, ML Firdaus, I Rahayu, YA El-Badry, EE Hussein and ZM El-Bahy. Photocatalytic phenol degradation by silica-modified titanium dioxide. *Appl. Sci.* 2021; **11**, 9033.
[36] KJ Stevenson. Review of originpro 8.5. *J. Am. Chem. Soc.* 2011; **133**, 5621.

[37] H Zheng, H Svengren, Z Huang, Z Yang, X Zou and M Johnsson. Hollow titania spheres loaded with noble metal nanoparticles for photocatalytic water oxidation. *Microporous Mesoporous Mater.* 2018; **264**, 147-50.
[38] J Duan, Y Liu, X Pan, Y Zhang, J Yu, K Nakajim and H Taniguchi. High photodegradation efficiency of rhodamine B catalyzed by bismuth silicate nanoparticles. *Catal. Commun.* 2013; **39**, 65-9.
[39] MA Abdel-Rahman, Y Tashiro and K Sonomoto. Recent advances in lactic acid production by microbial fermentation processes. *Biotechnol. Adv.* 2013; **31**, 877-902.
[40] MR Samarghandi, M Zarrabi, MN Sepehr, R Panahi and M Foroghi. Removal of acid red 14 by pumice stone as a low-cost adsorbent: Kinetic and equilibrium study. *Iran. J. Chem. Chem. Eng.* 2013; **31**, 19-27.
[41] AE Nogueira, E Longo, ER Leite and ER Camargo. Synthesis and photocatalytic properties of bismuth titanate with different structures via oxidant peroxo method (OPM). *J. Colloid Interface Sci.* 2014; **415**, 89-94.
[42] LZ Pei, HD Liu, N Lin and HY Yu. Bismuth titanate nanorods and their visible light photocatalytic properties. *J. Alloys Compd.* 2015; **622**, 254-61.
[43] Z Chen, H Jiang, W Jin and C Shi. Enhanced photocatalytic performance over $Bi_4Ti_3O_{12}$ nanosheets with controllable size and exposed {001} facets for rhodamine B degradation. *Appl. Catal. B: Environ.* 2016; **180**, 698-706.
[44] P Dumrongrojthanath, T Thongtem, A Phuruangrat and S Thongtem. Synthesis and characterization of hierarchical multilayered flower-like assemblies of Ag doped Bi_2WO_6 and their photocatalytic activities. *Superlattices Microstruct.* 2013; **64**, 196-203.